European Journal of Human Genetics (2010) 18, 1107–1113

www.nature.com/ejhg

ARTICLE

CAMOS, a nonprogressive, autosomal recessive, congenital cerebellar ataxia, is caused by a mutant zinc-finger protein, ZNF592

Elsa Nicolas[1,2,4], Yannick Poitelon[1,4], Eliane Chouery[2], Nabiha Salem[2], Nicolas Levy[1,3], André Mégarbané[1,2] and Valérie Delague*[,1]

CAMOS (Cerebellar Ataxia with Mental retardation, Optic atrophy and Skin abnormalities) is a rare autosomal recessive syndrome characterized by a nonprogressive congenital cerebellar ataxia associated with mental retardation, optic atrophy, and skin abnormalities. Using homozygosity mapping in a large inbred Lebanese Druze family, we previously reported the mapping of the disease gene at chromosome 15q24–q26 to a 3.6-cM interval between markers *D15S206* and *D15S199*. Screening of candidate genes lying in this region led to the identification of a homozygous p.Gly1046Arg missense mutation in *ZNF592*, in all five affected individuals of the family. *ZNF592* encodes a 1267-amino-acid zinc-finger (ZnF) protein, and the mutation, located within the eleventh ZnF, is predicted to affect the DNA-binding properties of ZNF592. Although the precise role of ZNF592 remains to be determined, our results suggest that ZNF592 is implicated in a complex developmental pathway, and that the mutation is likely to disturb the highly orchestrated regulation of genes during cerebellar development, by either disrupting interactions with target DNA or with a partner protein.
European Journal of Human Genetics (2010) **18,** 1107–1113; doi:10.1038/ejhg.2010.82; published online 9 June 2010

Keywords: CAMOS; missense mutation; *ZNF592*; C2H2 zinc-finger domain; cerebellar ataxia; nonprogressive

INTRODUCTION

Nonprogressive congenital ataxias (NPCAs) are a small group of disorders, accounting for ~10% of nonprogressive infantile encephalopathies.[1] Clinically, NPCA manifests in infancy with abnormal motor development, hypotonia, and delayed ability to sit and stand, followed by the appearance of ataxia.[1] Dysarthria, mental retardation, and spasticity are also often present.[2] Pathologically, most of the congenital ataxias are characterized by hypoplasia or atrophy of parts of the cerebellum and brain stem.[3] It has been estimated that 50% of cases of congenital ataxias and mental retardation are genetically determined, most of them being of autosomal recessive inheritance.[4] To date, ~17 loci responsible for NPCA are known, of which 14 are of autosomal recessive transmission. When excluding the nine loci responsible for Joubert's syndrome, five loci are assigned to autosomal recessive NPCA: Cayman ataxia (MIM 601238) at chromosome 19p13.3,[5] due to mutations in *ATCAY* (MIM 608179),[6] Cerebellar ataxia 3 (SCAR6) at chromosome 20q11–q13 (MIM 608029),[7] disequilibrium syndrome at chromosome 9p24 (MIM 224050),[8] 'Norman-type' ataxia (SCAR2 or CLA1) at chromosome 9q34–9qter (MIM 213200),[9] and CAMOS (Cerebellar Ataxia with Mental retardation, Optic atrophy and Skin abnormalities) (SCAR5) at chromosome 15q24–q26.[10]

ZNF592 is a 1267-amino-acid (aa) zinc-finger (ZnF) protein, predicted to contain 13 classical C2H2-type ZnF domains. C2H2 ZnFs were first discovered in the transcription factor IIIA from *Xenopus laevis*[11] and constitute one of the most common DNA-binding motifs found in eukaryotes.[12] C2H2-ZnF proteins usually have a crucial role as transcriptional regulators by mediating interactions between DNAs and proteins[11] and perform various functions in cellular processes, such as transcription, translation, metabolism, and signaling by binding to nucleic acids or proteins.[13,14]

In this study, we report the identification of a missense mutation in *ZNF592*, encoding a novel, highly conserved, ZnF transcription factor, as the pathogenic mutation causing CAMOS, a rare NPCA syndrome, wherein cerebellar ataxia is associated with mental retardation, optic atrophy, and skin abnormalities.[15]

MATERIALS AND METHODS

Patients

We previously published the localization of CAMOS to chromosome 15q24–q26 in a large consanguineous Lebanese family (Figure 1).[10] Briefly, all patients share the following clinical features: severely delayed developmental milestones, severe psychomotor retardation, proportionate short stature, cerebellar spastic ataxia, microcephaly, optic atrophy, speech defect, ultrastructural skin abnormalities, and cerebellar atrophy, most probably of prenatal onset. For a fully detailed clinical description of the patients, see the study by Mégarbané *et al*[15]

After informed consent was obtained from all individuals and parents of children included in this study, EDTA blood samples were collected and genomic DNA was extracted from lymphocytes using standard methods. Taken

[1]INSERM UMR_S 910, 'Génétique Médicale et Génomique Fonctionnelle', Faculté de Médecine de la Timone, Université de la Méditerranée, Marseille, France; [2]Unité de Génétique Médicale, Faculté de Médecine, Université Saint-Joseph, Beirut, Lebanon; [3]AP-HM, Département de Génétique Médicale, Hôpital d'enfants Timone, Marseille, France
*Correspondence: Dr V Delague, INSERM UMR_S 910, 'Génétique Médicale et Génomique Fonctionnelle', Faculté de Médecine de la Timone, Université de la Méditerranée, 27 Boulevard Jean Moulin, 13385 Marseille Cedex 05, France. Tel: +33 4 91 78 68 94; Fax: +33 4 91 80 43 19; E-mail: valerie.delague@univmed.fr
[4]These authors contributed equally to this work.
Received 2 November 2009; revised 6 April 2010; accepted 21 April 2010; published online 9 June 2010

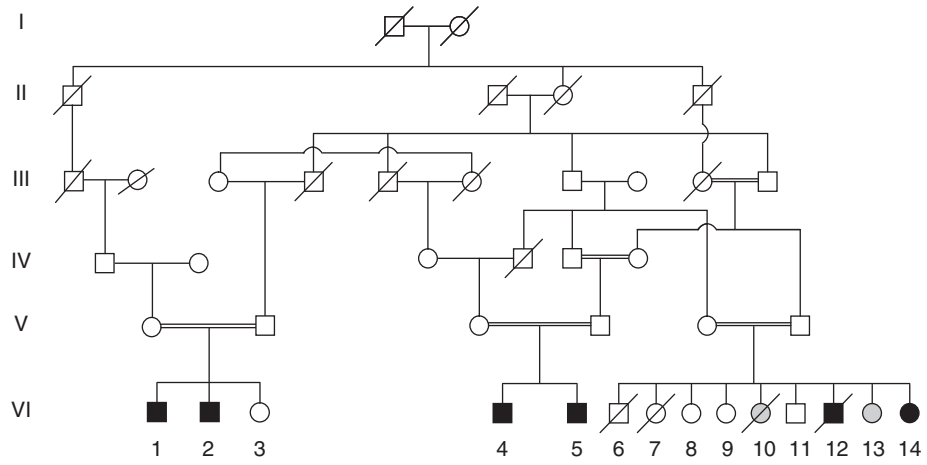

Figure 1 Pedigree of the Lebanese family. Blackened symbols indicate the affected individuals. Gray circles indicate patients affected with diastrophic dysplasia, which is another autosomal recessive disease segregating in this pedigree.

together, 15 DNA samples were collected for the study, including 5 affected individuals (Figure 1). All protocols performed in this study complied with the ethics guidelines of the institutions involved.

Mutation analysis

Of the 24 candidate genes present in the 3.6-cM homozygous interval, as described in the databases (Ensembl Genome Browser, UCSC Human Genome Browser), the following 10 were selected, based on their function and tissue-specific expression, and were tested for the presence of a pathogenic mutation: *AP3B2*, *SH3GL3*, *BTBD1*, *HMG20A*, *HOMER2*, *RKHD3*, *EFTUD1*, *ZSCAN2*, *SCAND2*, and *ZNF592* (Figure 2a). Exploration of the entire coding sequence and of exon–intron boundaries and 5′ as well as 3′ untranslated regions (UTRs), was performed for each candidate gene (Figure 2a). Intronic primers were designed using the Primer3 and OLIGOS v.9.3 software. Primer sequences and annealing temperatures used for PCRs are available in Supplementary material Table 1. DNA sequences were obtained from the UCSC Human Genome Browser (UCSC, March 2006 freeze), by comparing genomic DNA with cDNA sequences. Genomic DNA from patient VI.14 and a control were amplified under standard PCR conditions. All PCR-amplified fragments were analyzed by dHPLC/WAVE (Transgenomic, Omaha, NE, USA) and fluorescently sequenced in both directions, using an ABI 310 or ABI 3130 automated sequencer (Applied Biosystems, Foster City, CA, USA), for those presenting abnormal elution profiles (conditions for dHPLC analysis are available upon request). Chromatograms were compared with reference sequences using Sequencher v4.2 (Gene Codes Corporation, Ann Arbor, MI, USA) and ChromasPro v1.33 (Technelysium, Tewantin, Australia).

Segregation in the pedigree, of the identified c.3136G>A nucleotide change and its presence in 444 Lebanese control chromosomes, were assessed by PstI restriction endonuclease digestion (Roche Applied Sciences, Basel, Switzerland) or dHPLC.

Transcriptional analysis

Total RNA was extracted from freshly isolated lymphocytes or immortalized lymphocytes, using standard protocols as described before.[16] cDNAs were obtained from total RNA using Superscript I Reverse Transcriptase (Invitrogen Life Technologies, Carlsbad, CA, USA) and random primers (Invitrogen Life Technologies), in accordance with the recommendations of the supplier. cDNAs were then PCR amplified as described above. Primers and annealing temperatures for amplification of the whole *ZNF592* cDNA are available in Supplementary material Table 1. Primers corresponding to fragment 6 were used for verification of the effect of the variation on *ZNF592* splicing.

Semi-quantitative RT-PCR

In human adult tissues, the expression profile of *ZNF592* was characterized, using Rapid Scan Gene Expression Panels from Origene (Rockville, MD, USA). These panels consist of cDNAs synthesized from poly(A+) RNA and immobilized at four cDNAs concentrations (100× and 1000×) on a 96-well PCR plate. Human panels include 24 different human adult tissues and 12 brain tissues (Supplementary Figure 1a and b). The expression of *ZNF592* during development was assessed in six human fetal tissues by semi-quantitative RT-PCR using Multiple-Choice cDNAs from Origene, and, in mouse, using mRNAs extracted from whole embryo, at different developmental stages (Supplementary Figure 1d and e).

Primers used for amplification are listed in Supplementary material Table 1. In all experiments, β-actin was used for normalization and amplified using primers included in the kit (Origene).

Northern blot

Quantitative northern blot analysis of *ZNF592* expression in different human tissues was realized using commercially available synthetic polyA+ membranes from Ambion (Foster City, CA, USA) and Clontech (Moutain View, CA, USA), that were hybridized with a 972 bp radioactively labeled ([^{32}P]-dATP) cDNA probe, covering *ZNF592* exons 3–8. A human β-actin cDNA probe provided by the manufacturer (Origene) was used as a normalizing control.

For patients' northern blot, we immobilized polyA+ mRNAs, extracted from homozygous patient VI.1's, heterozygous father V.2's and Lebanese control's lymphoblastoid cells, using the μMacs mRNA isolation kit from Myltenyi Biotech (Bergisch Gladbach, Germany); and the obtained synthetic membrane was hybridized to the 972-bp *ZNF592* cDNA probe cited above. All steps were realized using the NorthernMax-Gly kit (Ambion), following the manufacturer's recommendations.

Quantitative real-time RT-PCR

SYBR Green real-time PCRs (quantitative real-time RT-PCR (QRT-PCRs)) were realized according to standard protocols in a 20-μl amplification mixture containing 10 μl of SYBR Green PCR Master Mix buffer (Applied Biosystems, Foster City, CA, USA), 0.25 μM of each primer, and 20 ng of RNAse H-treated (Invitrogen Life Technologies) cDNAs obtained from reverse transcription of 5 μg of DNAse I-treated total RNA extracted from homozygous patient VI.1, heterozygous father V.2, and controls blood lymphocytes using the High-Capacity cDNA Archive Kit (Applied Biosystems). Reactions were performed and data collected on the ABI PRISM 7500 Sequence Detection System (Applied Biosystems) using conditions recommended by the manufacturer. Each assay included nontemplate controls and the unknown samples in triplicate: that is, patient VI.1 and heterozygous father V.2. For *ZNF592*, five different calibrators (Lebanese controls) were used. All experiments were repeated twice, with a freshly extracted mRNA from patient VI.1 and father V.2. The expression values of *ZNF592* were normalized to that of *GUS* and *GAPDH*, whereas *CCDN1* and *CCDN2* expression values were normalized to that of *TBP* and *GUS*. For each gene, the expression ratio for a sample was

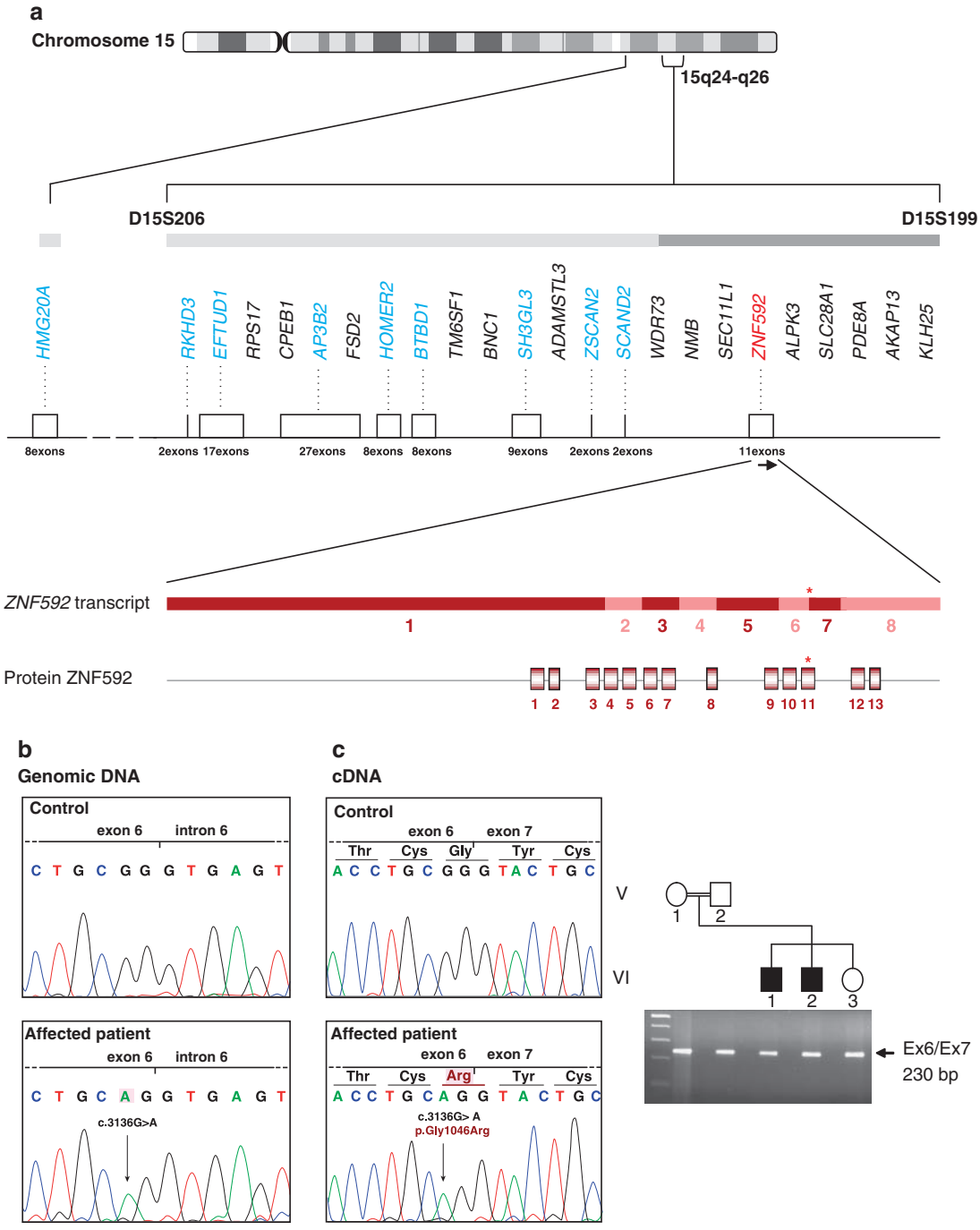

Figure 2 Candidate genes in the homozygous region identified in CAMOS with identification of mutations in *ZNF592*. (**a**) Chromosomal region at 15q24–q26 containing the CAMOS candidate locus as previously identified,[10] covering a 5.7-Mb (3.6-cM) region located between STR markers D15S206 (AFM299yf9) and D15S199 (AFM107×g7). The 24 known genes lying in this region are schematically represented, with candidate genes tested in our study indicated in blue. *ZNF592* is represented in red. *ZNF592* is located at chromosome 15q25.3, covering a genomic region of ~20 kb, and is transcribed in the direction centromere to telomere, as indicated by the black arrow. In the transcript of *ZNF592*, coding exons are represented in red and pink. *ZNF592* is composed of 8 exons and the transcript is 4312-bp long (Acc. number BC094688), with a coding sequence of 3804 bp (exons 1–8). In the protein ZNF592, the 13 C2H2 zinc-finger (ZnF) domains are represented by boxes. Location of the mutation identified in this study is indicated by an asterisk in exon 6 of the gene, or in the eleventh ZnF of the protein. (**b**) Chromatograms showing the c.3136G>A mutation identified in *ZNF592* exon 6 in Lebanese patients. Lebanese control sequence is shown in a control. (**c**) Effect of the mutation on the transcription: agarose gel migration showing a transcript of normal size in the patients. Chromatograms showing the absence of small deletions/insertions and the c.3136G>A missense mutation giving rise to the replacement of a glycine by an arginine in the protein (p.Gly1046Arg).

calculated as the ratio between the average *mRNA* signal in the patient and the signal from calibrators. After the reaction, the data were analyzed using the comparative CT relative quantification method using the ABI PRISM 7500 system SDS software version 1.2.3 (Applied Biosystems). Primers for QRT-PCR were designed using Primer Express software version 2 (Applied Biosystems). All primer sequences are listed in Supplementary material Table 1.

Results are presented as average values for experiments with *GUS* as a normalizing gene.

Protein homology modeling studies

Wild-type and mutant eleventh ZNF592's C2H2 ZnFs were modelized using freely available Swiss-Pdb Viewer software. As no Protein Data Bank (PDB) structure was available for ZNF592 in the PDB, we used the structure of the C2H2 zinc-binding domain from ZFP64/ZNF338 (PDB ID: 1X5W), another human ZnF protein, presenting sequence homologies with ZNF592's ZnFs. Using Swiss-Pdb Viewer, we changed all aa to ZNF592 aa. In the mutant ZnF, the glycine at position 41 was replaced by an arginine, as observed in patients affected with CAMOS, who harbor the p.Gly1046Arg missense mutation.

In the mutant C2H2 ZnF domain 3D structure (B), the mutation of Gly41 to Arg41 results in the formation of a new hydrogen bond interaction between Arg41 and the adjacent tyrosine Tyr42.

RESULTS

Using DNA pooling and homozygosity mapping, we had previously assigned CAMOS to a 3.6-cM (5.7-Mb) homozygous region at chromosome 15q24–q26 between markers *D15S206* and *D15S199*, in a large consanguineous Lebanese family, with five affected individuals[10] (Figure 1). Screening of the coding sequence of genes lying in the candidate interval, by direct sequencing, allowed us to identify a c.3136G>A homozygous transition in exon 6 of *ZNF592*, a gene encoding a 1267-aa ZnF protein, and predicted to contain 13 classical C2H2-type ZnF domains (Figure 2). The c.3136G>A nucleotide change identified in our patients was not reported in the NCBI dbSNP database, segregated perfectly with the phenotype in the pedigree, and was not found in the 444 tested Lebanese control chromosomes, excluding the possibility that it might be a rare polymorphism and indicating that this variant was likely to be pathogenic. As the variation affected the second last nucleotide of exon 6, just upstream the 5′ consensus donor splice site, we tested whether it might affect the splicing of *ZNF592* transcript. RT-PCR studies using total RNAs extracted from patients and Lebanese control's blood lymphocytes, and primers located in exons surrounding *ZNF592* exon 6, allowed us to rule out this hypothesis, at least in the tested tissue (Figure 2c). Occurrence of small deletions/insertions was excluded by sequencing of the obtained RT-PCR fragment in patients and controls. Other complex splicing defects were excluded by amplification and sequencing of the entire cDNA. At the protein level, the *ZNF592* c.3136G>A mutation is likely to be a missense mutation, leading to the replacement of a glycine by an arginine at residue 1046 (p.Gly1046Arg; GGG>AGG). It targets a highly conserved aa residue among eutherian mammals, located in the eleventh C2H2 ZnF domain, at the base of the loop between the two conserved cysteines (Figure 3).

Protein homology modeling using wild-type and mutant predicted C2H2 ZnF domain 3D structure showed that mutation of glycine to arginine results in the formation of a new hydrogen bond interaction between Arg41 and the adjacent tyrosine Tyr42 in the mutant C2H2 ZnF (Figure 4).

Considering the specificity of tissues involved in our pathology (central nervous system (CNS) and skin), we characterized the expression profile of *ZNF592*, in both human and mouse tissues (Supplementary Figure 1). Both semi-quantitative RT-PCR experiments, using Rapid Scan Gene Expression Panels from Origene, and northern blot experiments demonstrated ubiquitous expression of *ZNF592* in all studied human adult tissues, notably in the brain and skin, with higher expression in skeletal muscle (Supplementary Figure 1a–c). In the CNS, *ZNF592* is expressed widely, including in the cerebellum and cerebellar vermis, with higher expression in the substantia nigra (Supplementary Figure 1b). Very low levels of *ZNF592* mRNA were detected in the ovary, uterus, and salivary glands (Supplementary Figure 1c). Finally, semi-quantitative RT-PCR experiments showed expression of *ZNF592* in six tested human fetal tissues and early expression of *Zfp592 (ZNF592* mouse ortholog) during development: as early as embryonic day E10 in whole mouse embryo (Supplementary Figure 1d–e). In the mouse brain, *Zfp592* mRNAs were detectable at birth (P0) and adult stages (Supplementary Figure 1e).

In patients affected with CAMOS, we analyzed the mRNA levels of *ZNF592* using northern blot and QRT-PCR. Both experiments evidenced higher levels of *ZNF592* transcript levels in both the patient and the heterozygous father, as compared with control (data not shown for northern blot and Supplementary Figure 2 for QRT-PCR), with a mean three-fold increase in patient VI.1. Surprisingly, *ZNF592* transcript levels were even higher in the heterozygous father. No statistical analysis could be performed because of the small size of the sample (only one patient); however, all experiments were performed in triplicate and were repeated twice, with freshly extracted total RNA samples in the second experiment. Unfortunately, we were unable to confirm these results at the protein level, as a polyclonal antibody against ZNF592 generated in rabbit failed to detect ZNF592 in control tissues (data not shown).

We studied the expression of cyclin-D1 (*CCND1*) and cyclin-D2 (*CCND2*) in CAMOS patient VI.1's lymphocytes using QRT-PCR. Interestingly, we found an increase in *CCND1* and *CCND2* mRNA levels, again, both in the patient and in the heterozygous father as compared with control, with a mean 43- and 3-fold increase in *CCND1* and *CCND2* patient's transcripts levels, respectively. As for *ZNF592*, no statistical analysis could be performed, but all experiments were performed in triplicate and were repeated twice.

DISCUSSION

CAMOS is a rare nonprogressive cerebellar ataxia syndrome, in which cerebellar ataxia is associated with mental retardation, optic atrophy, and skin abnormalities.[15] Since the first report and localization of the gene at chromosome 15q24–q26 in a large consanguineous Lebanese family,[10,15] no additional patients have been reported, pointing out the very low prevalence of this disease. In this study, we report the identification of a c.3136G>A missense mutation (p.Gly1046Arg) in *ZNF592*, in patients from this family. ZNF592 is a novel, highly conserved, 1267-aa ZnF protein, predicted to contain 13 classical C2H2-type ZnF domains (Figures 2a and 3a), which constitute one of the most common DNA-binding motifs found in eukaryotes.[12] Several genes encoding ZnF proteins have been implicated in human pathologies, such as *ZNF215* in Beckwith–Wiedemann syndrome[17] (MIM 130650); *ZNF41* (MIM 314995),[18] *ZNF81*[19] (MIM 314998), and *ZNF674*[20] (MIM 300573) in nonsyndromic, X-linked mental retardation or *ZNF750* in Seborrhea-like dermatitis with psoriasiform elements.[21] *ZNF592* is the first gene of this family found to be mutated in a cerebellar syndrome, although mutations have been described in *APTX* (MIM 606350), the gene mutated in oculomotor-apraxia (AOA1) and encoding aprataxin, a nuclear protein with a role in DNA repair and containing one C2H2 ZnF.[22,23]

The p.Gly1046Arg mutation identified in this study targets a highly conserved aa and is located within the eleventh ZnF of ZNF592. *In silico* protein homology modeling studies predict a destabilizing effect for the mutation, by the formation of a new hydrogen bond interaction between the mutated arginine and the adjacent tyrosine (Figure 4), thereby leading to the disruption of the ZnF, as described

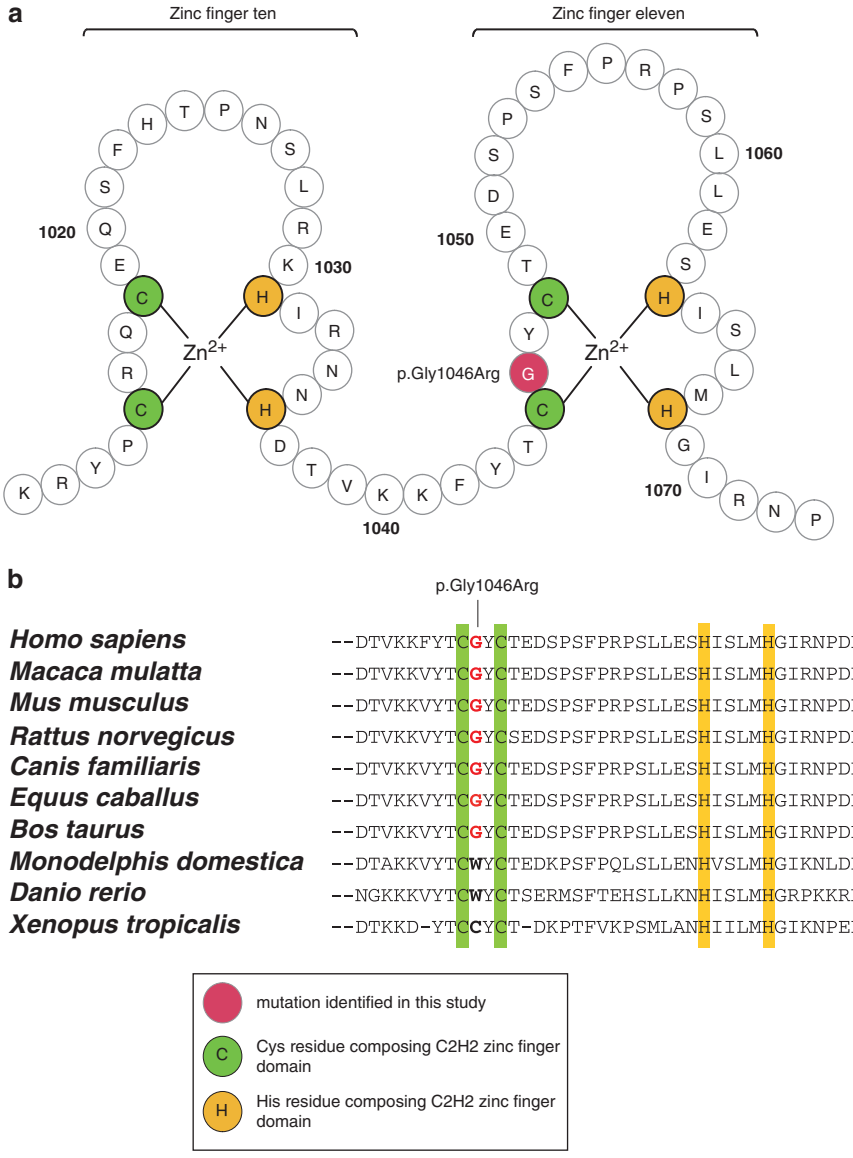

Figure 3 Schematic representation of the zinc fingers (ZnFs) and conservation between species. (**a**) Schematic representation of ZnFs 10 and 11, showing the location of the mutated glycine at residue 1046, at the base of the eleventh ZnF. (**b**) Multiple alignments between human ZNF592 protein and several orthologs. The glycine at residue 1046 mutated in our study is indicated in red and is highly conserved among eutherian mammals.

for other transcription factors.[24–26] By affecting the DNA-binding properties of ZNF592 or interactions with other TFs, the p.Gly1046Arg mutation in *ZNF592* might also regulate *ZNF592*'s own expression, as evidenced by the higher levels of *ZNF592* transcripts observed in the studied patient homozygous for the p.Gly1046Arg mutation. Thus, the ratio of wild-type *versus* mutant ZNF592 might be crucial, explaining the peculiar pattern of expression observed in heterozygote father *versus* homozygote patient.

The multiplicity of tissues/organs involved, as well as the non-progressive nature of CAMOS, is characteristic of a developmental disease, with abnormal development of the cerebellum as a hallmark. Several genes for congenital human cerebellar malformations have been identified to date, including members of the Zic family of C2H2 ZnF TFs.[27] Indeed, heterozygous deletions of the adjacent *ZIC1* (MIM 600470) and *ZIC4* (MIM 608948) genes cause Dandy–Walker malformation (MIM 220200), the most common human congenital cerebellar malformation,[27] and deletion of *Zic1* in mouse results in cerebellar malformations and axial skeletal abnormalities.[28] Zic genes have critical roles in various developmental processes and are regulated by a number of pathways/TFs. We postulate that ZNF592 might be a downstream or upstream element in the Zic-regulated pathways. By disrupting the interactions between ZNF592 and its target consensus sequence, or between ZNF592 TF and another TF (as described for Zic with members of the Gli family of C2H2 TFs[29,30]), the p.Gly1046Arg mutation identified in this study is likely to affect the pathways regulated by Zic genes. This hypothesis is supported by the early expression of *ZNF592*, as early as E10 (Supplementary Figure 1e), the nonprogressive nature of CAMOS, and the presence of a dilated fourth ventricle in CAMOS patients as observed in patients affected with Dandy–Walker malformation. CCND1 (MIM

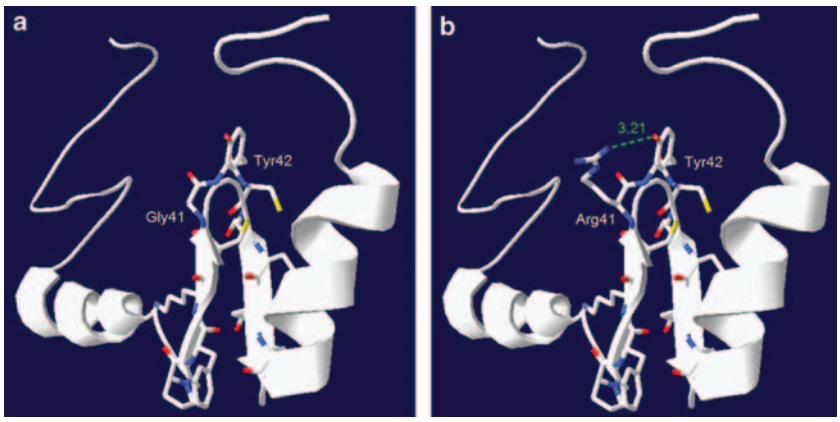

Figure 4 Three-dimensional structures of wild-type and mutant ZNF592 C2H2 zinc finger (ZnF). Wild-type (**a**) and mutant (**b**) eleventh C2H2 ZnF modeling using the freely available Swiss-Pdb Viewer software. In the mutant C2H2 ZnF domain 3D structure (panel b), the mutation of Gly41 to Arg41 results in the formation of a new hydrogen bond interaction between Arg41 and the adjacent tyrosine Tyr42.

168461), a downstream effector of Zic proteins,[31] shows reduced transcript expression levels in the cerebella of Zic mutants,[32] and mice lacking CCND1 and CCND2 (MIM 123833) (cyclin D3-only mice) lacked normally developed cerebella.[33] In our patient's lymphocytes, we observed an increase in *CCND1* and *CCND2* mRNA levels, especially important for *CCND1* (43-fold increase). Although preliminary, these results of altered expression patterns are extremely interesting and bring further support to the hypothesis of ZNF592, as a TF implicated in a complex developmental pathway. Indeed, D1-cyclin has been shown to be upregulated by Notch signaling,[34] known to inhibit differentiation of cerebellar granule neuron precursors by maintaining proliferation.[35] Abnormally elevated levels of CCND1 in cerebellar granule neuron precursors, by disrupting proliferation/differentiation processes in these cells, might have impaired cerebellar development in our patients. In this context, the surprisingly elevated levels of *ZNF592*, *CCND1* and *CCND2* transcripts in the heterozygous father (Supplementary Figure 2), are difficult to interpret, but might be explained by the fact that the regulation of the described pathways is highly orchestrated in time, and that the amount of each TF might change rapidly in time, with a combination of tightly regulated levels of expression.

In conclusion, this study describes the identification of *ZNF592* as the gene responsible for CAMOS, a rare, nonprogressive, cerebellar ataxia syndrome previously identified in a Lebanese family. Further studies have to be performed to elucidate the pathophysiological mechanisms underlying CAMOS. However, our results allow us to formulate the hypothesis that ZNF592 might be implicated in a complex developmental pathway, affecting several tissues, such as the 'Zic/Cyclin/Notch' pathway. A major argument in favor of the involvement of ZNF592 in this pathway is the presence, in our patients, of an inversion of the usual osmiophilic pattern of the vessels in skin biopsies: the endothelial cells (ECs) in patients are osmiophilic, compared with the normal endothelium, which is electrolucent.[15] Indeed, neural and vascular precursors use common signals and pathway, such as Notch, Sonic Hedgehog (Shh), or BMP, to specify their fate; and neural and vascular cells influence the cell-fate decision making of one another.[36] The Notch pathway, in particular, has a crucial role in arterial EC specification, by inducing arterial fate at the expense of venous EC fate.[36] Implication of ZNF592 in a pathway common to neural and vascular progenitors would explain the affection of both tissues in CAMOS.

The identification of ZNF592 as the defective protein in CAMOS constitutes a first step in the comprehension of the pathophysiological mechanisms underlying this syndrome. Further experiments must be conducted to better define which pathways are involved.

CONFLICT OF INTEREST

The authors declare no conflict of interest.

ACKNOWLEDGEMENTS

We express our deepest gratitude and sympathy to the families for their full cooperation throughout the study. We thank Professor Gérard Lefranc for constant support and logistics. This work was financially supported by the Saint-Joseph University (USJ) and the Institut National de la Santé et de la Recherche Médicale (Inserm). Elsa Nicolas was supported by a grant from the Agence Universitaire de la Francophonie (AUF).

WEB RESOURCES

The GenBank accession numbers are as follows:

AP3B2: NM_004644
SH3GL3: NM_003027
BTBD1: NM_025238
HMG20A: NM_018200
HOMER2: NM_199330
RKHD3: NM_032246
EFTUD1: NM_024580
ZSCAN2: NM_181877
SCAND2 : NM_033634 (the sequence was suppressed afterwards as the transcript is in fact an NMD transcript)
ZNF592: BC094688, NM_014630, NC_000015, ENST00000299927, ENSG00000166716.

In the databases, discrepancies exist between GenBank (NM_014630 and NC_000015), the UCSC Genome Browser, and the Ensembl browser (ENST00000299927, ENSG00000166716) regarding the length of the transcript (but not the CDS), the number of exons, the length of the UTRs, and the region covered by *ZNF592*. On the basis of the results of northern blot experiments (see Supplementary Figure 1c), we used the sequence with Acc. Number BC094688, as a reference in our study.

ZFP64/ZNF388: NP_060667
PDB ID for ZFP64/ZNF338: 1X5W

ZNF592 proteins were: NP_055445 (*Homo sapiens*), NP_848822 (*Mus musculus*), XP_001084237 (*Macaca mulatta*), NP_001099742 (*Rattus norvegicus*), XP_545869 (*Canis familiaris*), XP_001916274 (*Equus caballus*), NP_001095506 (*Bos taurus*), XP_001364673 (*Monodelphis domestica*), NP_001072160 (*Xenopus tropicalis*), NP_001038678 (*Danio rerio*).

The URLs used were as follows:

Online Mendelian Inheritance in Man (OMIM): http://www.ncbi.nlm.nih.gov/Omim.

The design of primers (Primer3 software) is available at http://frodo.wi.mit.edu/.

The UCSC Genome Browser is available at http://genome.ucsc.edu/cgi-bin/hgGateway.

Ensembl Server: http://www.ensembl.org/.

NCBI dbSNP database: http://www.ncbi.nlm.nih.gov/SNP/.

RCSB Protein Databank: http://www.rcsb.org/pdb/home/home.do.

Swiss-Pdb Viewer: http://spdbv.vital-it.ch/.

DEPP (Disorder Enhanced Phosphorylation predictor): http://www.pondr.com.

1 Steinlin M: Non-progressive congenital ataxias. *Brain Dev* 1998; **20**: 199–208.
2 Harding A: Hereditary ataxias and related disorders; in Asbury AK, McKhann GM, McDonald W(eds):: *Diseases of the Nervous System. Clinical Neurobiology.* Philadelphia: WB Saunders Company, 1992, 2nd edn, Vol 2, pp 1169–1178.
3 Harding A: Clinical features and classification of inherited ataxias; in Harding A, Deufel T (eds): *Advances in Neurology.* Raven Press Ltd, New York, 1993, Vol 61, pp 1–14.
4 Gustavson K, Hagberg B, Sanner G: Identical syndromes of cerebral palsy in the same family. *Acta Paediatr Scand* 1969; **58**: 330–340.
5 Nystuen A, Benke P, Merren J, Stone E, Sheffield V: A cerebellar ataxia locus identified by DNA pooling to search for linkage disequilibrium in an isolated population from the Cayman Island. *Hum Mol Genet* 1996; **5**: 525–531.
6 Bomar JM, Benke PJ, Slattery EL *et al*: Mutations in a novel gene encoding a CRAL-TRIO domain cause human Cayman ataxia and ataxia/dystonia in the jittery mouse. *Nat Genet* 2003; **35**: 264–269.
7 Kvistad PH, Dahl A, Skre H: Autosomal recessive non-progressive ataxia with an early childhood debut. *Acta Neurol Scand Suppl* 1985; **71**: 295–302.
8 Boycott KM, Flavelle S, Bureau A *et al*: Homozygous deletion of the very low density lipoprotein receptor gene causes autosomal recessive cerebellar hypoplasia with cerebral gyral simplification. *Am J Hum Genet* 2005; **77**: 477–483.
9 Delague V, Bareil C, Bouvagnet P *et al*: A non-progressive autosomal recessive ataxia maps to chromosome 9q34-9qter in a large consanguineous Lebanese family. *Ann Neurol* 2001; **50**: 250–253.
10 Delague V, Bareil C, Bouvagnet P *et al*: A new autosomal recessive non-progressive congenital cerebellar ataxia, associated with optic atrophy and mental retardation, maps to chromosome 15q24-q26 in a large consanguineous Lebanese Druze family. *Neurogenetics* 2002; **4**: 23–27.
11 Miller J, McLachlan AD, Klug A: Repetitive zinc-binding domains in the protein transcription factor IIIA from Xenopus oocytes. *EMBO J* 1985; **4**: 1609–1614.
12 Bouhouche N, Syvanen M, Kado CI: The origin of prokaryotic C2H2 zinc finger regulators. *Trends Microbiol* 2000; **8**: 77–81.
13 Gamsjaeger R, Liew CK, Loughlin FE, Crossley M, Mackay JP: Sticky fingers: zinc-fingers as protein-recognition motifs. *Trends Biochem Sci* 2007; **32**: 63–70.
14 Pabo CO, Peisach E, Grant RA: Design and selection of novel Cys2His2 zinc finger proteins. *Annu Rev Biochem* 2001; **70**: 313–340.
15 Mégarbané A, Delague V, Ruchoux M *et al*: A new autosomal recessive cerebellar ataxia disorder in a large inbred Lebanese family. *Am J Med Genet* 2001; **101**: 135–141.
16 Delague V, Jacquier A, Hamadouche T *et al*: Mutations in FGD4 encoding the Rho GDP/GTP exchange factor FRABIN cause autosomal recessive Charcot-Marie-Tooth type 4H. *Am J Hum Genet* 2007; **81**: 1–16.
17 Alders M, Ryan A, Hodges M *et al*: Disruption of a novel imprinted zinc-finger gene, ZNF215, in Beckwith-Wiedemann syndrome. *Am J Hum Genet* 2000; **66**: 1473–1484.
18 Shoichet SA, Hoffmann K, Menzel C *et al*: Mutations in the ZNF41 gene are associated with cognitive deficits: identification of a new candidate for X-linked mental retardation. *Am J Hum Genet* 2003; **73**: 1341–1354.
19 Kleefstra T, Yntema HG, Oudakker AR *et al*: Zinc finger 81 (ZNF81) mutations associated with X-linked mental retardation. *J Med Genet* 2004; **41**: 394–399.
20 Lugtenberg D, Yntema HG, Banning MJ *et al*: ZNF674: a new kruppel-associated box-containing zinc-finger gene involved in nonsyndromic X-linked mental retardation. *Am J Hum Genet* 2006; **78**: 265–278.
21 Birnbaum RY, Zvulunov A, Hallel-Halevy D *et al*: Seborrhea-like dermatitis with psoriasiform elements caused by a mutation in ZNF750, encoding a putative C2H2 zinc finger protein. *Nat Genet* 2006; **38**: 749–751.
22 Moreira MC, Barbot C, Tachi N *et al*: The gene mutated in ataxia-ocular apraxia 1 encodes the new HIT/Zn-finger protein aprataxin. *Nat Genet* 2001; **29**: 189–193.
23 Date H, Onodera O, Tanaka H *et al*: Early-onset ataxia with ocular motor apraxia and hypoalbuminemia is caused by mutations in a new HIT superfamily gene. *Nat Genet* 2001; **29**: 184–188.
24 Smith JF, Hawkins J, Leonard RE, Hanas JS: Structural elements in the N-terminal half of transcription factor IIIA required for factor binding to the 5S RNA gene internal control region. *Nucleic Acids Res* 1991; **19**: 6871–6876.
25 Necela BM, Cidlowski JA: A single amino acid change in the first zinc finger of the DNA binding domain of the glucocorticoid receptor regulates differential promoter selectivity. *J Biol Chem* 2004; **279**: 39279–39288.
26 Aarnisalo P, Santti H, Poukka H, Palvimo JJ, Janne OA: Transcription activating and repressing functions of the androgen receptor are differentially influenced by mutations in the deoxyribonucleic acid-binding domain. *Endocrinology* 1999; **140**: 3097–3105.
27 Grinberg I, Northrup H, Ardinger H, Prasad C, Dobyns WB, Millen KJ: Heterozygous deletion of the linked genes ZIC1 and ZIC4 is involved in Dandy-Walker malformation. *Nat Genet* 2004; **36**: 1053–1055.
28 Merzdorf CS: Emerging roles for zic genes in early development. *Dev Dyn* 2007; **236**: 922–940.
29 Millen KJ, Gleeson JG: Cerebellar development and disease. *Curr Opin Neurobiol* 2008; **18**: 12–19.
30 Koyabu Y, Nakata K, Mizugishi K, Aruga J, Mikoshiba K: Physical and functional interactions between Zic and Gli proteins. *J Biol Chem* 2001; **276**: 6889–6892.
31 Aruga J: The role of Zic genes in neural development. *Mol Cell Neurosci* 2004; **26**: 205–221.
32 Aruga J, Inoue T, Hoshino J, Mikoshiba K: Zic2 controls cerebellar development in cooperation with Zic1. *J Neurosci* 2002; **22**: 218–225.
33 Ciemerych MA, Kenney AM, Sicinska E *et al*: Development of mice expressing a single D-type cyclin. *Genes Dev* 2002; **16**: 3277–3289.
34 Ronchini C, Capobianco AJ: Induction of cyclin D1 transcription and CDK2 activity by Notch(ic): implication for cell cycle disruption in transformation by Notch(ic). *Mol Cell Biol* 2001; **21**: 5925–5934.
35 Solecki DJ, Liu XL, Tomoda T, Fang Y, Hatten ME: Activated Notch2 signaling inhibits differentiation of cerebellar granule neuron precursors by maintaining proliferation. *Neuron* 2001; **31**: 557–568.
36 Carmeliet P: Blood vessels and nerves: common signals, pathways and diseases. *Nat Rev Genet* 2003; **4**: 710–720.

Supplementary Information accompanies the paper on European Journal of Human Genetics website (http://www.nature.com/ejhg)